



OPEN ACCESS

EDITED BY

Komuraiah Myakala,
Georgetown University Medical Center,
United States

REVIEWED BY

Ramdas Bhat,
Department of Pharmacology at Srinivas
College of Pharmacy, India
Sandrine Ettou,
Ingenia Therapeutics, United States

*CORRESPONDENCE

Xiaoqin Wang,
✉ wangxiaoqin@hbhtcm.com

†These authors have contributed equally to
this work and share first authorship

RECEIVED 03 August 2024

ACCEPTED 30 July 2025

PUBLISHED 09 September 2025

CITATION

Wang L, Li H, Guo X and Wang X (2025) Integrative RNA-seq and CLIP-seq analysis reveals *hnRNP-F* regulation of *TNF α /NF κ B* signaling in high-glucose conditions. *Front. Physiol.* 16:1475441.
doi: 10.3389/fphys.2025.1475441

COPYRIGHT

© 2025 Wang, Li, Guo and Wang. This is an open-access article distributed under the terms of the [Creative Commons Attribution License \(CC BY\)](#). The use, distribution or reproduction in other forums is permitted, provided the original author(s) and the copyright owner(s) are credited and that the original publication in this journal is cited, in accordance with accepted academic practice. No use, distribution or reproduction is permitted which does not comply with these terms.

Integrative RNA-seq and CLIP-seq analysis reveals *hnRNP-F* regulation of *TNF α /NF κ B* signaling in high-glucose conditions

Lan Wang^{1,2,3,4†}, Huimeng Li^{1†}, Xinyuan Guo¹ and Xiaoqin Wang^{2,3,4*}

¹Hubei University of Chinese Medicine, Wuhan, China, ²Hubei Provincial Hospital of Traditional Chinese Medicine, Wuhan, China, ³Affiliated Hospital of Hubei University of Chinese Medicine, Hubei Key Laboratory of Theory and Application Research of Liver and Kidney in Traditional Chinese Medicine, Wuhan, China, ⁴Hubei Shizhen Laboratory, Wuhan, China

Background: Diabetic kidney disease (DKD), with its complex pathogenesis, is the most important cause of end-stage renal disease and has become an urgent public health problem worldwide. Heterogeneous nuclear ribonucleoprotein F (*hnRNP-F*) is a member of a subfamily of widely expressed nuclear heterogeneous ribonucleoproteins with biological roles in regulating gene expression and variable splicing. Some studies have investigated *hnRNP-F* in DKD. However, its potential mechanism in renal intrinsic cells has rarely been reported. Therefore, it is necessary to further investigate its potential mechanism in DKD in the search for novel ideas for new therapeutic targets for DKD.

Methods: In this study, *hnRNP-F* was overexpressed in human renal proximal tubular epithelial (HK-2) cells cultured in high-glucose conditions, while an empty vector was transfected into HK-2 cells as a control group (NC). Meanwhile, to avoid any osmotic stress that might be caused by the use of high sugar, we also added mannose as a non-osmotic control. RNA-seq was utilized to generate transcriptome data following *hnRNP-F* overexpression, allowing for the analysis of differential gene expression and alternative splicing events influenced by *hnRNP-F* overexpression. Similarly, we overexpressed *hnRNP-F* in mouse podocyte clone 5 (MPC5) cells and verified the relevant indicators using Western blotting (WB) under high-glucose and high-mannitol conditions, respectively. We also downloaded the CLIP-seq data of *hnRNP-F* in human 293T cells from the Gene Expression Omnibus (GEO) database. Through integrative analysis of RNA-seq and CLIP-seq, we tried to identify a set of potential direct targets of *hnRNP-F* in cells.

Results: In this study, RNA sequencing (RNA-seq) was utilized to demonstrate that the upregulation of *hnRNP-F* in HK-2 cells cultured under high-glucose conditions resulted in a substantial decrease in the expression of genes associated with the inflammatory response and suppression of the *TNF α /NF κ B* signaling pathway. This was also verified in MPC5 cells. By analyzing CLIP-seq and RNA-seq data, we found that *hnRNP-F* may inhibit gene expression by binding to lncRNA *SNHG1*. Conversely, this upregulation led to a significant increase in alternative splicing events of genes implicated in DKD, such as

hnRNPA2B1, *OSML*, *UGT2B7*, *TRIP6*, and *IRF3*. Combining CLIP-seq data, we found that *hnRNP-F* binds to and regulates variable splicing of the *hnRNP* protein family and splicing factors. This result suggests that *hnRNP-F* may regulate alternative splicing through the coordinated action of multiple splicing factors.

Conclusion: *hnRNP-F* has dual functions in mRNA transcriptional and post-transcriptional levels and may bind with lncRNA *SNHG1* to negatively regulate the transcription of genes involved in the *TNF α /NF κ B* signaling pathway. Meanwhile, *hnRNP-F* may function in the co-regulation of alternative splicing events in cells by interacting with ZFP36 to form a complex.

KEYWORDS

hnRNP-F, diabetic kidney disease, RNA-seq, differential gene expression, variable splicing, *TNF α -NF κ B* signaling pathway

1 Introduction

Diabetic kidney disease (DKD) is a global public health problem and an important cause of chronic kidney disease (CKD), leading to end-stage renal disease, and urgently needs our in-depth research and effective response (Chen et al., 2020; Barrera-Chimal and Jaisser, 2020). Various factors are implicated in DKD progression, including autoimmunity, inflammation, renal fibrosis, renal hemodynamic alterations, mitochondrial dysfunction, abnormalities in glucolipid metabolism, oxidative stress, and epigenetic inheritance (Tuttle et al., 2022; Lin et al., 2018). Therefore, drugs targeting inflammatory and fibrotic pathways have important therapeutic implications in DKD research (Lytvyn et al., 2020).

Heterogeneous nuclear ribonucleoprotein F (*hnRNP-F*) is a subfamily of widely expressed *hnRNPs*. The proteins of this subfamily are RNA-binding proteins (RBPs) that interact with heterogeneous nuclear RNAs. In addition, as splicing factors, *hnRNPs* are involved in various aspects of RNA metabolism, including alternative splicing of target RNAs, polyadenylation, sequence editing, RNA transport, RNA stabilization and degradation, intracellular localization, and translational control (Smith et al., 2021; Huang et al., 2017; Ladd, 2016). Alternative splicing (AS) is a major mechanism for generating multiple structurally and functionally different proteins from a single gene, greatly expanding proteome diversity (Cheng et al., 2021). In humans, approximately 95% of multiexon genes undergo AS, and a recent study demonstrated that splice isoform switching is critical in the various kidney diseases, especially in DKD (Zhou et al., 2024; Liao et al., 2024).

Based on the biological role of *hnRNP-F* in regulating gene expression and AS, its role in DKD has gradually received attention. At present, scholars have confirmed the closer link between *hnRNP-F* and DKD to varying degrees in various experiments. For example, in patients with type 2 diabetes, the protein levels of *hnRNP-F* have significantly decreased in renal cortex tissues. It shows that *hnRNP-F* is involved in mediating insulin inhibition of Bcl2 modifier expression and diabetic tubulopathy (Ghosh et al., 2019). *hnRNP-F* protects the kidney from oxidative stress and nephropathy by stimulating Sirtuin-1 expression and signaling in diabetic mice (Ghosh et al., 2019). Overexpression of *hnRNP-F* attenuates *TGF- β 1*-induced diabetic kidney injury in mice, mainly by stimulating renal Ace-2 gene expression (Lo et al., 2015). *hnRNP-F* was

recently found to have a protective effect against podocyte injury, and *hnRNP-F* deficiency promotes podocyte pathology through activation of Mettl14 expression and inhibition of Sirt1 expression by its nuclear translocation (Liao et al., 2024).

In the study of DKD, HK-2 cells, as a model of human proximal tubular epithelial cells, are widely used to investigate the mechanisms of diabetes-induced tubular damage and potential therapeutic strategies (Darshi et al., 2024). In the present study, renal tubular epithelial cells (HK2) overexpressing *hnRNP-F* were cultured in high-glucose conditions, while a control group (NC) was similarly exposed to high-glucose. Mannitol was added to the media as an osmotic control. Subsequently, transcriptome data were acquired through RNA sequencing (RNA-seq) following the overexpression of *hnRNP-F* under high-glucose conditions. The expression of differentially expressed genes linked to inflammation was confirmed in both db/db and db/m mouse models. Additionally, overexpression of *hnRNP-F* in conditionally immortalized mouse podocyte cell line (Clone 5) (MPC5) confirmed its inhibitory effect on the *TNF- α /NF- κ B* inflammatory signaling pathway. This approach enabled the analysis of differential gene expression and AS events influenced by the overexpression of *hnRNP-F*. Furthermore, the anti-inflammatory effect of *hnRNP-F* has been experimentally demonstrated under LPS stimulation. The results show that *hnRNP-F* broadly regulates gene expression and alternative splicing related to diabetic nephropathy, particularly in inflammation-related pathways, offering new insights into DKD gene regulation.

2 Materials and methods

2.1 Cell lines and cell culture

HK-2 cells (Cell Bank of China Academy of Sciences) were cultured in DMEM/F12 (Gibco) supplemented with 10% FBS (Gibco) and 1% penicillin/streptomycin (MilliporeSigma). MPC-5 cells (Procell) were maintained in RPMI 1640 (Procell) containing 10% FBS (Gibco) and 1% penicillin/streptomycin (MilliporeSigma). Both cell lines were incubated at 37 °C under 5% CO₂. Upon reaching 50% confluence, cells were treated with 30 mM high-glucose (HG; MilliporeSigma) for 72 h. Mannitol (MilliporeSigma) served as an osmotic control. LPS (Solarbio) was dissolved in sterile PBS to prepare a 10-mg/mL stock solution. HK-2 cells (10 µg/mL)

and MPC5 cells (45 µg/mL) were treated with these LPS solutions for 24 h to model cell injury. Cells were subsequently harvested for Western blot analysis of target protein expression.

2.2 *hnRNP-F* was overexpressed in HK-2 and MPC5 cell lines

We employed four parallel wells for each group of HK-2 cells: HK-2 cells transfected with the control lentivirus were cultured in a high-glucose medium containing 30 mM glucose (HG-NC) for 72 h, while a separate group of control lentivirus-transfected HK-2 cells was cultured in a medium containing 30 mM mannitol to serve as an osmotic control (OS-NC). Similarly, HK-2 cells transfected to overexpress the *hnRNP-F* lentivirus (Gene ID:98758, Lentiviral expression vector LV5) were maintained in a 30 mM glucose medium (HG-OE) and in a mannitol medium (OS-OE) for 72 h, respectively. MPC5 cells were cultured under HG conditions (30 mM, 72 h), mannitol treatment (30 mM, 72 h), or LPS stimulation (10 µg/mL, 24 h) and then transfected with an *hnRNP-F* overexpressing plasmid packaged in a lentiviral vector (Gene ID: 98758, vector name: HBLV-ZsGreen-PURO).

2.3 Reverse transcription quantitative real-time PCR (RT-qPCR)

Total RNA was isolated from the renal cortex and cells separately using the TRIzol method, and 1 µL of total RNA was used as the template, reverse-transcribed to cDNA, and continued to be amplified by using cDNA as the template, sequentially, at 95 °C for 3 min, 1 cycle, 95 °C for 10 s, and 62 °C for 40 s, for a total of 40 cycles. The mRNA levels of HG-NC and HG-OE were determined using the $2^{-\Delta\Delta CT}$ method, with β -actin and GAPDH serving as internal references. Similarly, mRNA levels in renal tissues of *db/db* and *db/m* mice were calculated. The specific primer sequences are shown in Table 1.

2.4 Co-immunoprecipitation (Co-IP)

After extracting the proteins from the cells OE-*hnRNP-F* and the NC HK-2 cells, the lysates were pre-cleared with rabbit IgG (3 µg/mg protein) and protein A/G magnetic beads. Then, they were incubated overnight at 4 °C with anti-*hnRNP-F* or control IgG (3 µg/mg protein). The complexes were captured with fresh magnetic beads (20 µL/500 µL lysate, room temperature for 2 h), washed three times with lysis buffer, and eluted in 1× Laemmli buffer (95 °C, 5 min) for immunoblotting.

2.5 Western blotting analysis

Total protein lysates (30 µg/lane) from cells or renal tissues were separated by 10% SDS-PAGE and transferred to PVDF membranes (Millipore). After blocking with 5% non-fat milk/TBST for 1 hour, the membranes were incubated overnight at 4°C with the following primary antibodies: *hnRNP-F*, β -actin, GAPDH (1:5000;

Proteintech, 67701-1-Ig, 20536-1-AP, 60004-1-Ig), *p-p65* (1:500; Invitrogen, MA5-15160), *p65* (1:5000; Abclonal, A19653) and *TNF- α* (1:1000; Abcam, ab183218). Following TBST washes (3 × 10 min), membranes were incubated 1 h with HRP-conjugated secondary antibodies: Goat anti-mouse, Goat anti-rabbit (1:1000; Proteintech, SA00001-1, SA00001-2). Signals were detected by ECL (Proteintech, P0018S) and quantified using ImageJ (NIH, v1.53e), normalized to β -actin/GAPDH.

2.6 RNA extraction and sequencing

All RNA was processed with RQ1 DNase (Promega) to remove DNA. The quality and quantity of the purified RNA were determined by measuring the absorbance at 260 nm/280 nm (A260/A280) utilizing SmartSpec Plus (BioRad). RNA integrity was further verified by 1.5% agarose gel electrophoresis.

For each sample, 1 µg of total RNA was used for RNA-seq library preparation. mRNAs were captured by VAHTS mRNA capture beads (Vazyme, N401). The purified RNA was treated with RQ1 DNase (Promega) to remove DNA before being used for directional VAHTS with a Universal V8 RNA-seq Library Prep Kit for Illumina (NR605). Polyadenylated mRNAs were purified and fragmented. Fragmented mRNAs were converted into double-stranded cDNA. Following end repair and A tailing, the DNAs were ligated to Adapter (N323). After purification of the ligation product and size fractioning to 300–500 bps, the ligated products were amplified and purified, then quantified and stored at -80 °C before sequencing. The strand marked with dUTP (the second cDNA strand) is not amplified, allowing strand-specific sequencing.

For high-throughput sequencing, the libraries were prepared following the manufacturer's instructions and applied to an Illumina NovaSeq 6000 system for 150-nt paired-end sequencing.

2.7 RNA-seq raw data cleaning and alignment

First, raw reads containing more than 2-N bases were discarded. Then, adapters and low-quality bases were trimmed from raw sequencing reads using FASTX-Toolkit (Version 0.0.13). The short reads less than 16 nt were dropped as well. Afterward, clean reads were aligned to the GRCh38 genome by HISAT2 (Kim et al., 2015), allowing four mismatches. Uniquely mapped reads were used for gene read number counting and FPKM calculation (fragments per kilobase of transcript per million fragments mapped) (Trapnell et al., 2010).

2.8 Differentially expressed genes (DEG) analysis

The R Bioconductor package DESeq2 was applied to screen out the differentially expressed genes (DEGs) (Love et al., 2014). The P-value for correction <0.05 and fold change ≥ 2 or ≤ 0.5 were set as the cut-off criteria for identifying DEGs.

TABLE 1 Primer sequences for qRT-PCR.

Gene	Forward primer (5'-3')	Reverse primer (5'-3')
HOMO- <i>hnRNP-F</i>	CTCCGTCGTGGAAGCAGG	CGAGCAGGACTGGTTCTGT
HOMO- <i>GAPDH</i>	TCGGAGTCACGGATTTGGT	TTCCCGTTCTCAGCCTTGAC
HOMO- <i>β-actin</i>	CACCCAGCACAATGAAGATCAAGAT	CCAGTTTTAAATCCTGAGTCAAGC
Mouse- <i>hnRNP-F</i>	GCCTCGTTCAGTTGCCTC	AATGCCAATGTACCTCCGGG
Mouse- <i>GAPDH</i>	AACGACCCCTTCATTGAC	GAAGACACCAGTAGACTCCAC
Mouse- <i>β-actin</i>	TGTACCCAGGCATTGCTGAC	AACGCAGCTCAGTAACAGTCC
Mouse- <i>GDF15</i>	GCAGACTTATGATGACCTGGTGG	AAGGGGAGTGTAGGTGAGGAGC
Mouse- <i>IL6</i>	CCCCAATTCCAATGCTCTCC	CGCACTAGGTTGCCGAGTA
Mouse- <i>PTX3</i>	CTCAGTCCCAGTCCCTAGTGTG	GGAGTCCACCCCTCAGGAACAGA
Mouse- <i>TFPI2</i>	CTCCAGTCCAAAGGATGAAGGT	AGTTATTCTCATTCCCACACAGC
Mouse- <i>GAPDH</i>	CCTCGTCCCGTAGACAAAATG	TGAGGTCAATGAAGGGTCGT
Mouse- <i>β-actin</i>	TGGTCTTCTGGTGCCTGTCTC	CAGTCAGTATGTTCGGCTTCC

2.9 Batch effect correction and quality control

To minimize potential batch effects and technical variability in RNA-seq data, we applied ComBat_seq, an empirical Bayes method implemented in the “suva” R package, to adjust for known batch information across samples while preserving biological variance. Prior to batch correction, principal component analysis (PCA) was performed to visualize sample clustering and assess batch-related variation. After correction, PCA and hierarchical clustering confirmed improved consistency within experimental groups.

2.10 Alternative splicing analysis

The AS events and regulated alternative splicing events (RAS) between OE-*hnRNP-F* and NC samples were defined and quantified by using the splice sites usage variation analysis (SUVA) pipeline as described previously. Differential splicing of each pair of cells was analyzed. The frequency and reads proportion of the SUVA AS event (pSAR) of each AS event were calculated. For alternative splicing validation, we performed *RT-qPCR* on independent samples ($n = 3$ biological replicates) to confirm SUVA predictions, reporting both p-values and AS ratios in supplementary GraphPad data.

2.11 Functional enrichment analysis

In order to sort out functional categories of DEGs, Gene Ontology (GO) terms and KEGG pathways were identified using the KOBAS 2.0 server (Xie et al., 2011). The hypergeometric test and

the Benjamini–Hochberg FDR controlling procedure were used to define the enrichment of each term.

2.12 Gene set enrichment analysis (GSEA)

GSEA is an analytical method for genome-wide expression profile microarray data. By comparing genes with predefined gene sets, it can identify functional enrichment. A gene set means a group of genes sharing localization, pathways, functions, or other features. GSEA was conducted using the clusterProfiler package (version 4.6.2). The fold change of gene expression between the Mets group and the Primary group was calculated, and the gene list was generated in accordance with the change of $|\log_2\text{FC}|$. Afterward, we utilized GSEA-based enriched HALLMARK gene sets of the Molecular Signature Database.

2.13 CLIP-seq data analysis

Public sequence data files of CLIP-seq data of *hnRNP-F* in human 293T cells from GSE34993 were downloaded from the Sequence Read Archive (SRA). After reads were aligned onto the genome, only uniquely mapped reads were used for the following analysis. The “ABLIRC” strategy was used to identify the binding regions of RBP on the genome (Xia et al., 2017). Reads with at least 1-bp overlap were clustered as peaks. For each gene, computational simulation was used to randomly generate reads with the same number and lengths as reads in peaks. The output reads were further mapped to the same genes to generate random max peak heights from overlapping reads. The whole process was repeated 500 times. All the observed peaks with heights higher than those of random

max peaks (${}^*P < 0.05$) were selected. The target genes of *hnRNP-F* were finally determined by the peaks, and the binding motifs were called by HOMER software (Heinz et al., 2010).

2.14 Other statistical analyses

Principal component analysis (PCA) was performed by the R package factoextra (<https://cloud.r-project.org/package=factoextra>) to show the clustering of samples with the first two components. After controlling the reads by tags per million (TPM) of each gene in samples, an in-house script (sogen) was used for visualization of next-generation sequence data and genomic annotations. The pheatmap package (<https://cran.r-project.org/web/packages/pheatmap/index.html>) in R was used to perform the clustering based on Euclidean distance.

2.15 Animal experiments

Seven-week-old male *db/db* mice (C57BLKS/J background, 12 weeks old, mean body weight: 45.2 ± 3.1 g) and their *db/m* littermates were purchased from GemPharmatech Co., Ltd. (Chengdu, China) and maintained in the specific pathogen-free (SPF) animal facility at Hubei University of Chinese Medicine (Wuhan, China). All experimental procedures involving animals were performed in strict compliance with the institutional guidelines and approved by the Animal Ethics Committee of Hubei University of Chinese Medicine (Approval No. HUCMS00303837). DKD modeling success was defined by (1) fasting blood glucose ≥ 16.7 mmol/L for three consecutive tests, (2) urine output $> 150\%$ of controls, and (3) persistent proteinuria (Wang et al., 2021).

2.16 Statistical analysis

All results are presented as the average value plus or minus the standard deviation (SD). Statistical analyses were performed using GraphPad Prism 10.1.2 software (GraphPad, San Diego, CA). Differences between experimental groups were evaluated using either a paired two-tailed Student's t-test or one-way ANOVA followed by Bonferroni's *post hoc* test for multiple comparisons. A P-value of ≤ 0.05 was considered statistically significant.

3 Results

3.1 Effect of high-glucose on *hnRNP-F* protein level in HK2 cells

In cells treated under normal glucose and hypertonic conditions, there was no significant difference in *hnRNP-F* protein levels between the two groups ($P > 0.05$). However, in HK-2 cells cultured with HG concentrations, *hnRNP-F* levels were significantly reduced (${}^{**}P < 0.01$) (Figures 1A–C). Western blot analysis demonstrated that high-glucose downregulated *hnRNP-F* expression. Mannitol, used as an osmotic control, exhibited no significant effect

on *hnRNP-F* gene expression. Consistent with protein-level observations, RT-qPCR confirmed significant upregulation of *hnRNP-F* mRNA in high-glucose-treated HK-2 cells (${}^*P < 0.05$ vs. control) (Figures 1D,E), while treatment with equiosmolar mannitol showed no comparable effect ($P > 0.05$).

3.2 Overexpression of *hnRNP-F* regulates gene expression in high-glucose-treated renal tubular epithelial cells

Overexpression of *hnRNP-F* was constructed in HK2 cells cultured in a HG environment. qPCR results showed that *hnRNP-F* gene expression levels were upregulated in HK-2 cells after infection with overexpression of the *hnRNP-F* lentivirus (Figure 2A). To comprehensively investigate the *hnRNP-F*-mediated transcriptional regulation in high-glucose (HG) conditions, we constructed cDNA libraries prepared from control and *hnRNP-F*-overexpression cells (three biological replicates), which were incubated in high-glucose and mannitol. After removing adapters and contaminating sequences, we obtained a total of 742.7 million high-quality reads from each sample (Supplementary Table S2). Approximately 91.2%–96.39% paired-end reads per sample were then aligned to the human GRCH38 genome. RNA-seq yielded robust expression for 18,051 genes (Supplementary Table S3). PCA was carried out and revealed excellent clustering of expression gene changes between the OE-*hnRNP-F* HK-2 cells and control samples for different treatment conditions (Figure 2B). To evaluate the dynamics of gene expression between OE-*hnRNP-F* vs. Ctrl cells, we compared expression among all pairwise combinations of the samples using DESeq2 (Love et al., 2014).

OE-*hnRNP-F* affects many gene expressions under HG conditions. A total of 890 DEGs were obtained (P -value of < 0.05 , fold change ≥ 2 , or ≤ 0.5 , FDR ≤ 0.05), of which 568 genes were upregulated and 322 genes were downregulated (Supplementary Table S4). Mannitol treatment was found to affect the expression of some genes (Supplementary Table S5), while the number of DEGs was larger in HK-2 cells treated with high-glucose than in HK-2 cells treated with mannitol. A Venn diagram illustrating the profiles of DEGs reveals an overlap between glucose and mannitol treatment (Figure 2C). This analysis displays unique and overlapping sets of DEGs in *hnRNP-F* overexpressing cells under HG treatment. Venn diagram analysis revealed an intersection of 118 genes between the high-glucose-treated and mannitol-treated OE-*hnRNP-F* HK-2 cells. Mannitol did not drastically affect overall gene expression when used as an osmolar control treatment.

To correlate the *hnRNP-F*-regulated gene expression and biological functions under high-glucose, we subjected all 890 DEGs to GO annotation (Supplementary Tables S6, S7). In the biological processes (BPs) of GO analysis, the upregulated genes in the OE-*hnRNP-F* samples were highly enriched in the “extracellular matrix organization” and “cell adhesion” processes (Figure 2D). The downregulated genes were mainly enriched in the inflammatory response and other related biological processes, as well as “regulation of insulin secretion,” “response to ischemia,” “regulation of insulin secretion,” “positive regulation of angiogenesis,” and “response to hypoxia,” which are closely related to the pathogenesis of DKD

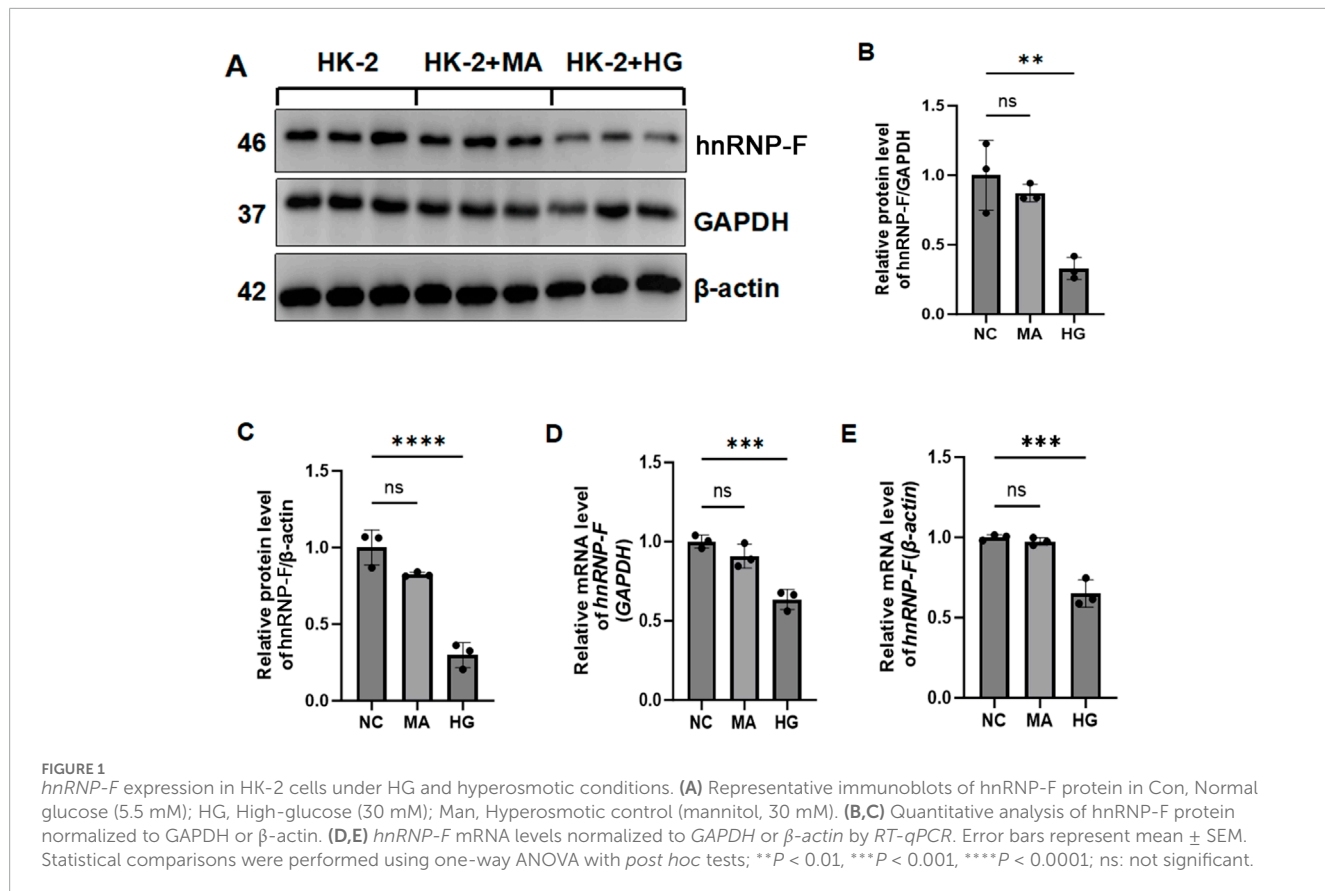


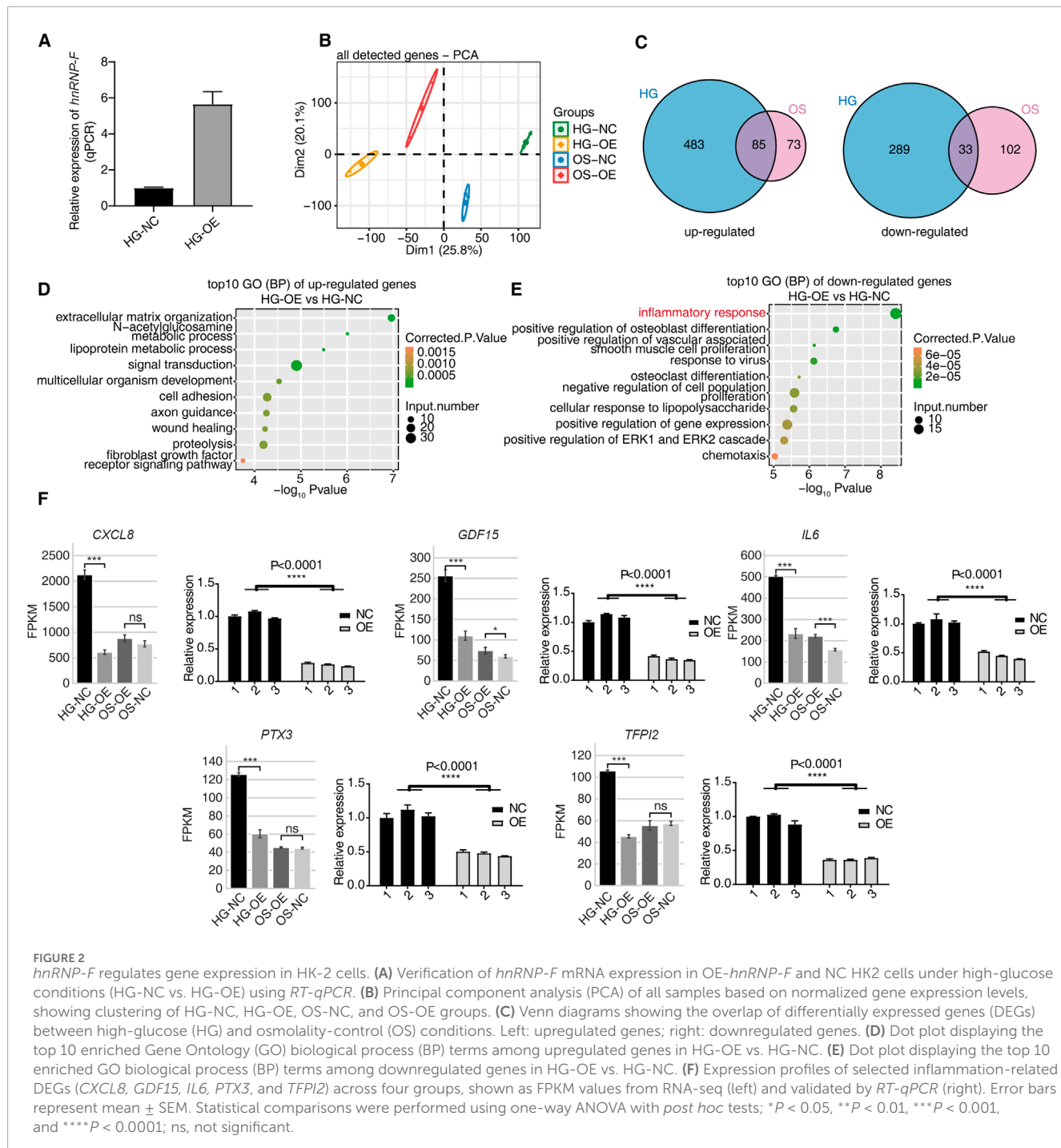
(Figure 2E; Supplementary Table S7). Among these, the decreased expression of inflammation-related genes was of particular interest. Representative genes from inflammatory-related genes (*CXCL8*, *IL6*, *GDF15*, *PTX3*, and *TFPI2*) were selected for RT-qPCR validation of their mRNA levels. *CXCL8* and *IL6* were found to be enriched in the tumor necrosis factor pathway (Supplementary Table S6). KEGG pathway enrichment analysis was also performed (Supplementary Figures S1A,B; Supplementary Table S8). The downregulated genes were also enriched in the *TNF* signaling pathway (Supplementary Figure S1B). The GO enrichment pathway of differentially expressed genes following mannitol treatment in HK-2 cells with *hnRNP-F* overexpression differs from that observed under HG conditions (Supplementary Figures S1C,D). Compared with HK-2 cells treated with HG and transfected with the empty vector (HG-NC group), overexpression of *hnRNP-F* could significantly downregulate the expression of *CXCL8*, *IL6*, *GDF15*, *PTX3*, and *TFPI2* (**** P < 0.0001). The qPCR results were consistent with RNA sequencing data (Figure 2F). The primers are listed in Supplementary Table S1. In the hyperosmotic mannitol control condition, the overexpression of *hnRNP-F* resulted in the significant downregulation of only two genes, *IL6* and *GDF15*. This suggests that the upregulation of *hnRNP-F* under normoglycemic conditions did not exert any significant effect. However, under hyperglycemic conditions, it led to a marked reduction in the expression of genes associated with the inflammatory response, particularly those involved in the *TNF* signaling pathway and the pathogenesis of DKD.

3.3 Overexpression of *hnRNP-F* downregulates the transcription of genes involved in the *TNF* signaling pathway under HG conditions

We performed GSEA of genes differentially expressed upon *hnRNP-F* overexpression under high-glucose. The overexpression of *hnRNP-F* resulted in a significant inhibition of the *TNF α /NF κ B* signaling pathway (Figure 3A). As demonstrated in Figure 3B, the upregulation of *hnRNP-F* resulted in a notable decrease in the expression of *PTX3* and *IL6*, both of which are genes associated with the *TNF α /NF κ B* signaling pathway. Even in the hypertonic control of mannitol, overexpression of *hnRNP-F* inhibited the expression of these genes. The findings indicated that the upregulation of *hnRNP-F* suppressed the transcription of genes associated with the *TNF* signaling pathway, such as *CXCL8*, *IL6*, and *PTX3*.

3.4 Identification that *hnRNP-F* regulates alternative splicing events in HK-2 cells under high-glucose conditions

Given the multi-functional nature of *hnRNP-F* as an RNA-binding protein, our analysis also encompasses the impact of *hnRNP-F* on the regulation of AS events. We obtained a total of 125 million uniquely mapped reads from each sample, in which 33.15%–44.04% were junction reads (Supplementary Table S2). We



analyzed the RNA-seq data using the software SUVA (9). Our analysis revealed the presence of distinct alternative splicing events (ASEs) and regulated alternative splicing events (RASEs) among the OE-*hnRNP-F* and control cells in the HG and mannitol-treated groups. Specifically, alt3p and alt5p were the main ASEs and RASEs between OE-*hnRNP-F* and control cells (Figure 4A; Supplementary Figure S3A; Supplementary Table S9). The SUVA-identified ASEs corresponded to the classical ASEs. *hnRNP-F* overexpression processing in HG cultured HK-2 cells resulted in a large number of differential variable splicing events, with

a total of 1,158 significant RASEs detected. The main variable splicing event types included 65 3pMXE, 66 5pMXE, 230 A3SS, 27 A3SS&ES, 177 A5SS, 52 A5SS&ES, 261 ES, 4 IntronR, 67 MXE, and 209 cassette exons (Figure 4B; Supplementary Table S9). Mannitol treatment mainly affects the AS events of A3SS and ES (Supplementary Figure S3B; Supplementary Table S9). Figure 3C illustrates the presence of novel splicing events among the RASEs under HG conditions, a finding that aligns with the results observed following mannitol treatment (Supplementary Figure S3C). These findings suggest that the overexpression of *hnRNP-F* can modulate

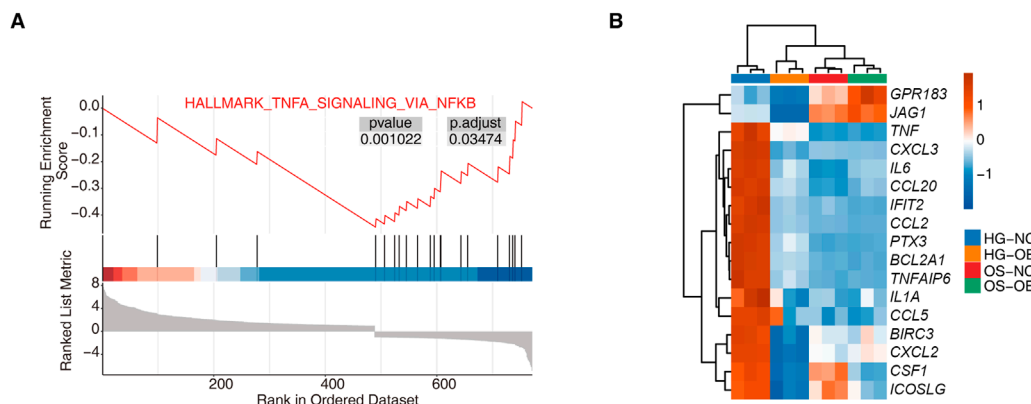


FIGURE 3
GSEA analysis for *hnRNP-F* overexpression in HK-2 cells. **(A)** Enrichment plot from gene set enrichment analysis (GSEA) showing significant negative enrichment of TNFa signaling via the NFkB pathway (HALLMARK_TNFA_SIGNALING_VIA_NFKB) in the HG-OE vs. the HG-NC group. **(B)** Hierarchical clustering heatmap showing the expression levels of TNFa/NFkB pathway-related genes across four sample groups: HG-NC, HG-OE, OS-NC, and OS-OE. Red and blue represent relative up- and downregulation, respectively.

intracellular alternative splicing in response to hypertonic treatment conditions.

Due to a splicing event involving two transcripts, which may account for a very small proportion of the entire gene expression, our study focused on identifying the more dominant transcripts in splicing events. We specifically quantified the number of splicing events with varying proportions of RASEs in the region covered by all reads. We also excluded splicing events with a low proportion (pSAR<50%). A total of 687 events with pSAR>50% were detected in overexpression *hnRNP-F* cells treated with high-glucose (Figure 4D). A total of 611 events were detected in the cells treated with mannitol (Supplementary Figure S3D). While a diversity of AS events was observed in cells treated with mannitol, the functional disparities in these splicing events between the two groups were pronounced when compared to the HG group. Notably, only 36 AS events were common to both treatment conditions (Figure 4E). This result indicated that overexpressed *hnRNP-F* HK-2 cells have a distinct AS profile in response to HG exposure. Gene Ontology biological process (GO-BP) enrichment analysis revealed that the HG group exhibited significant alterations in alternative splicing, predominantly enriched in pathways related to “regulation of RNA splicing” and “RNA splicing” (Figure 4F). The AS events of the mannitol group were mainly enriched in the “microvillus assembly” and “epithelial tube formation” pathway (Supplementary Figure S3E). To validate the accuracy of the predicted *hnRNP-F*-regulated ASEs selected from the RNA-seq data under the HG condition, two RASEs were selected for verification. The ratio of variable splicing events occurring in the gene *OSMR* (alt3p) decreased in the OE-*HNRNP-F* group (Figure 4H), and increased in the gene *TRIP6* (alt5p) (Figure 4G), as expected. We present the designed PCR primer pairs in Supplementary Table S1. *TRIP6* mediates inflammatory response and renal fibrosis in diabetic nephropathy (Lin et al., 2021).

3.5 *hnRNP-F* CLIP-seq reads revealed that *hnRNP-F* bound to splicing factors and regulated alternative splicing events

The *hnRNP-F* CLIP-seq data in human 293T cells were obtained from the SRA database accession number GSE34993. These data were utilized to identify transcripts that interact with *hnRNP-F* in cells. Only reads that mapped uniquely were included in the subsequent analysis. Comparisons between the control group and the IP groups revealed that the reads in the latter were predominantly enriched in noncoding exons, introns, and the 3'UTR region (Figure 5A). RNA-binding proteins that bind to the 3'UTR region often have an impact on RNA stability, suggesting that *hnRNP-F* may influence RNA stability.

Hypergeometric Optimization of Motif EnRichment (HOMER v4.11, <http://homer.ucsd.edu/homer/>) was employed for motif analysis of the specific binding peaks identified in the experimental samples. The motif enrichment analysis of the immunoprecipitation (IP) groups revealed enrichment of the UA-rich motif 5'-UUA-3' in the *hnRNP-F*-bound motif (Figure 5B). Subsequently, the gene sequences corresponding to the bound peak clusters were aligned with the GO database for annotation, which indicated enrichment in the RNA splicing process. These primarily included the heterogeneous ribonucleoprotein (HNRNP) family as well as SRSF splicing factors, including *HNRNPA2B1*, *HNRNPH*, *HNRNPU*, *SRSF1*, *SRSF5*, and *SRSF11* (Figure 5C). Studies have shown that *HNRNPA2B1*-binding motifs were UA rich (Wu et al., 2018).

Next, we asked whether differences in *hnRNP-F* binding genes were associated with different gene expressions. We performed gene-based differential binding analyses. We separately analyzed the transcriptome data of *hnRNP-F* in human 293T cells (GSE34995) and the transcriptome data of *hnRNP-F* in HK-2 cells that we independently measured. The results showed that *hnRNP-F*-binding

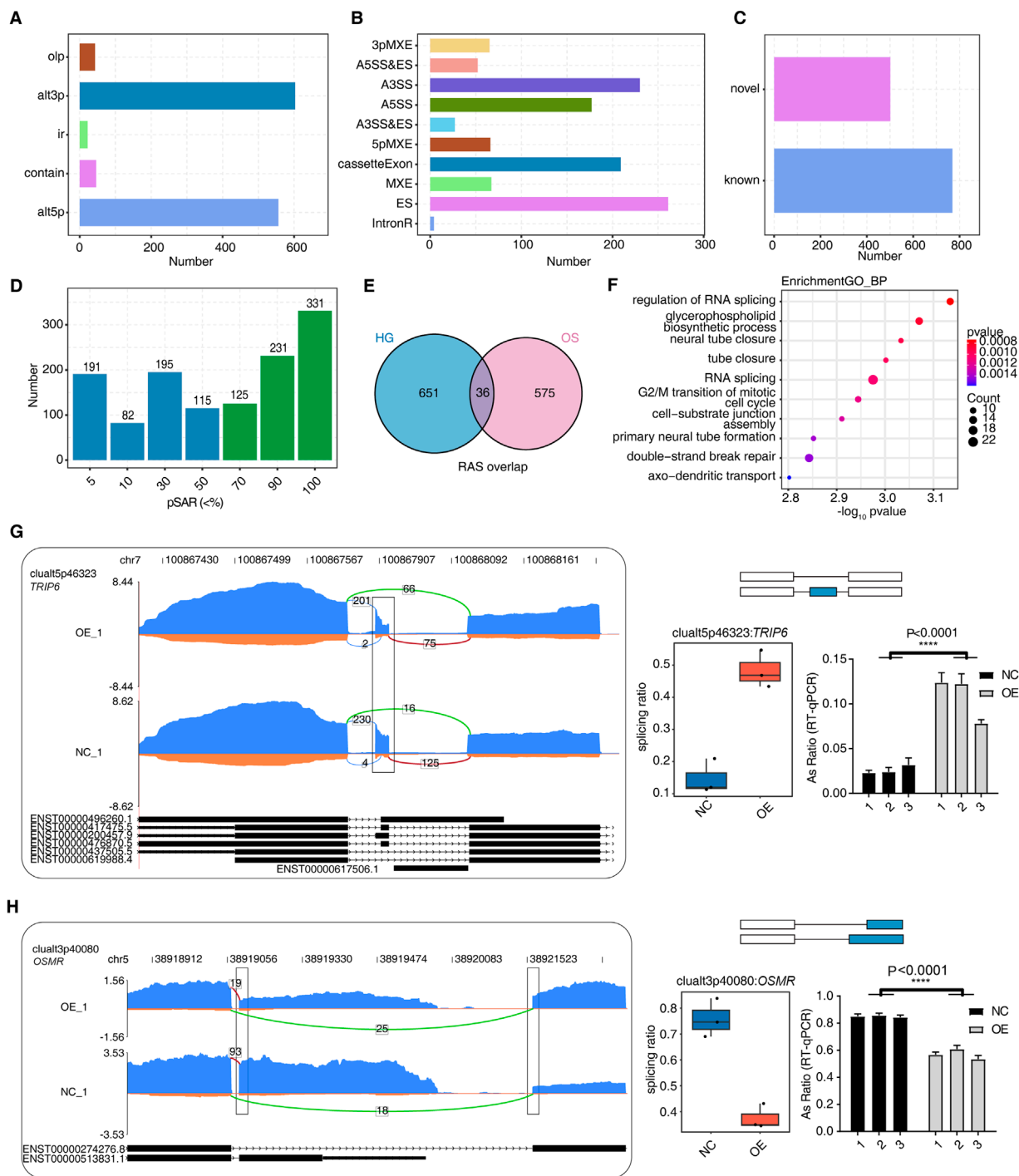
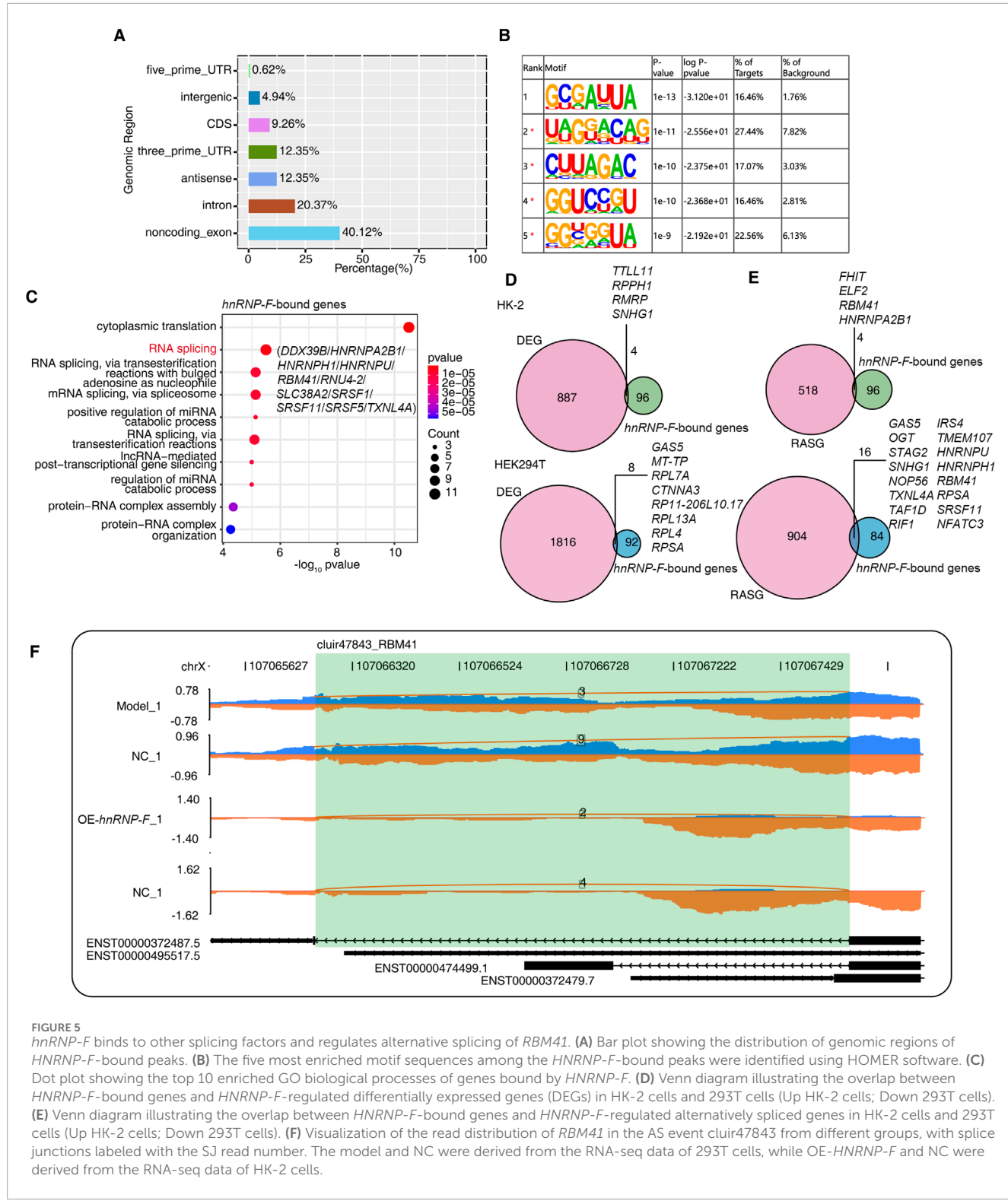
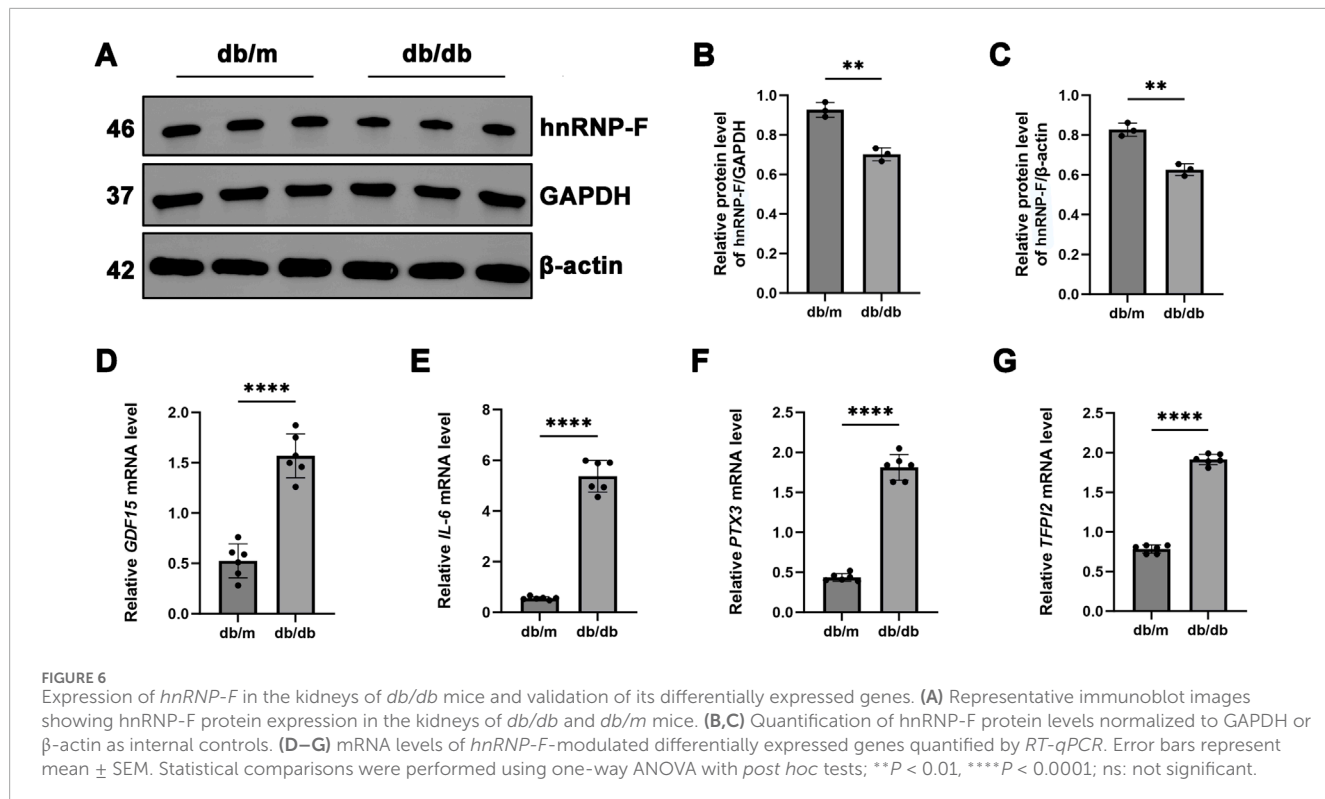


FIGURE 4
 hnRNP-F regulates alternative splicing events in HK-2 cells. **(A)** Bar plot showing the number of regulated alternative splicing (RAS) events among OE and NC samples detected by SUVA. **(B)** Bar plot categorizing splice junctions constituting RAS events detected by SUVA into classical alternative splicing (AS) event types and displaying the number of each type. **(C)** Bar plot showing the number of known and novel RAS events. **(D)** Bar plot showing the number of RAS events with different abundances (pSAR) among all RAS with a frequency $\geq 50\%$. RAS with pSAR $\geq 50\%$ are further analyzed and marked in red. **(E)** Venn diagram showing the overlap of high-confidence RAS events (pSAR $\geq 50\%$) identified under high-glucose (HG) and osmolality-control (OS) conditions. **(F)** The top 10 most enriched Gene Ontology (GO) terms related to biological processes are visualized for genes involved in RAS when comparing OE and NC samples. **(G)** Visualization of the read distribution of *TRIP6* in AS event clualt5p46323 from different groups, with splice junctions (SJs) labeled with SJ read numbers and the altered exon marked with a box. RNA-seq and RT-qPCR validation of the splicing ratio profile of the splicing event shown on the right. $****P < 0.0001$. **(H)** Visualization of the read distribution of *OSMR* in AS event clualt3p40080 from different groups, with splice junctions labeled with SJ read numbers and altered splice sites marked with a box. RNA-seq and RT-qPCR validation of the splicing ratio profile of the splicing event shown on the right. $****P < 0.0001$.



genes overlap with differently expressed genes. Of particular interest was the observation that the lncRNA *SNHG1*, when bound by *hnRNP-F* in 293T cells, exhibited differential expression in HK-2 cells overexpressing *hnRNP-F* (OE-*hnRNP-F*). Otherwise, in 293T cells, the lncRNA *SNHG1* underwent alternative splicing (Figures 5D,E). We also performed an association analysis utilizing

CLIP-seq and AS methodologies, which revealed that AS events occurred in four gene regions where *hnRNP-F* binds in HK-2 and in 16 gene regions in 293T cells (Figure 5E). The AS events of gene *RBM41* were detected in both cells (Figure 5E). The analysis of distribution maps indicated that the overexpression of *hnRNP-F* in HK-2 cells led to a diverse intron retention (ir) AS event of



RBM41. Similarly, in 293T cells with *hnRNP-F* knockdown, an ir AS event was also observed in *RBM41*. There is an *hnRNP-F* bound site near the splicing site (Figure 5F). The findings suggest that *hnRNP-F* can interact with *RBM41*. The interaction between *hnRNP-F* and *RBM41* results in the production of a truncated transcript of *RBM41*. Our hypothesis posits that the truncated transcript generated by *RBM41* could potentially influence the AS events. Nonetheless, given that the experiment conducted in 293T cells involved the knockdown of *hnRNP-F* and was characterized by a relatively low sequencing depth, this AS event warrants further experimental investigation.

3.6 Experimental validation of *hnRNP-F*-regulated differential gene expression in a *db/db* mouse model

Initially, we observed a significant reduction in the levels of *hnRNP-F* protein in the kidney of *db/db* mice compared to *db/m* controls ($^{****}P < 0.0001$) (Figures 6A–C). Subsequently, we validated the differentially expressed genes identified through RNA-seq (DEGs: *CXCL8*, *GDF15*, *IL6*, *PTX3*, and *TFPI2*) by *RT-qPCR*. Notably, *CXCL8* is a chemokine specific to humans and lacks a direct ortholog in mice, which precludes its validation in murine models. Compared to *db/m* controls, *db/db* mice demonstrated significantly elevated renal expression of genes associated with inflammation (*GDF15*, *IL6*, *PTX3*, and *TFPI2*, $^{****}P < 0.0001$) (Figures 6D–G), suggesting their critical roles in the progression of DKD. The downregulation of *hnRNP-F* protein

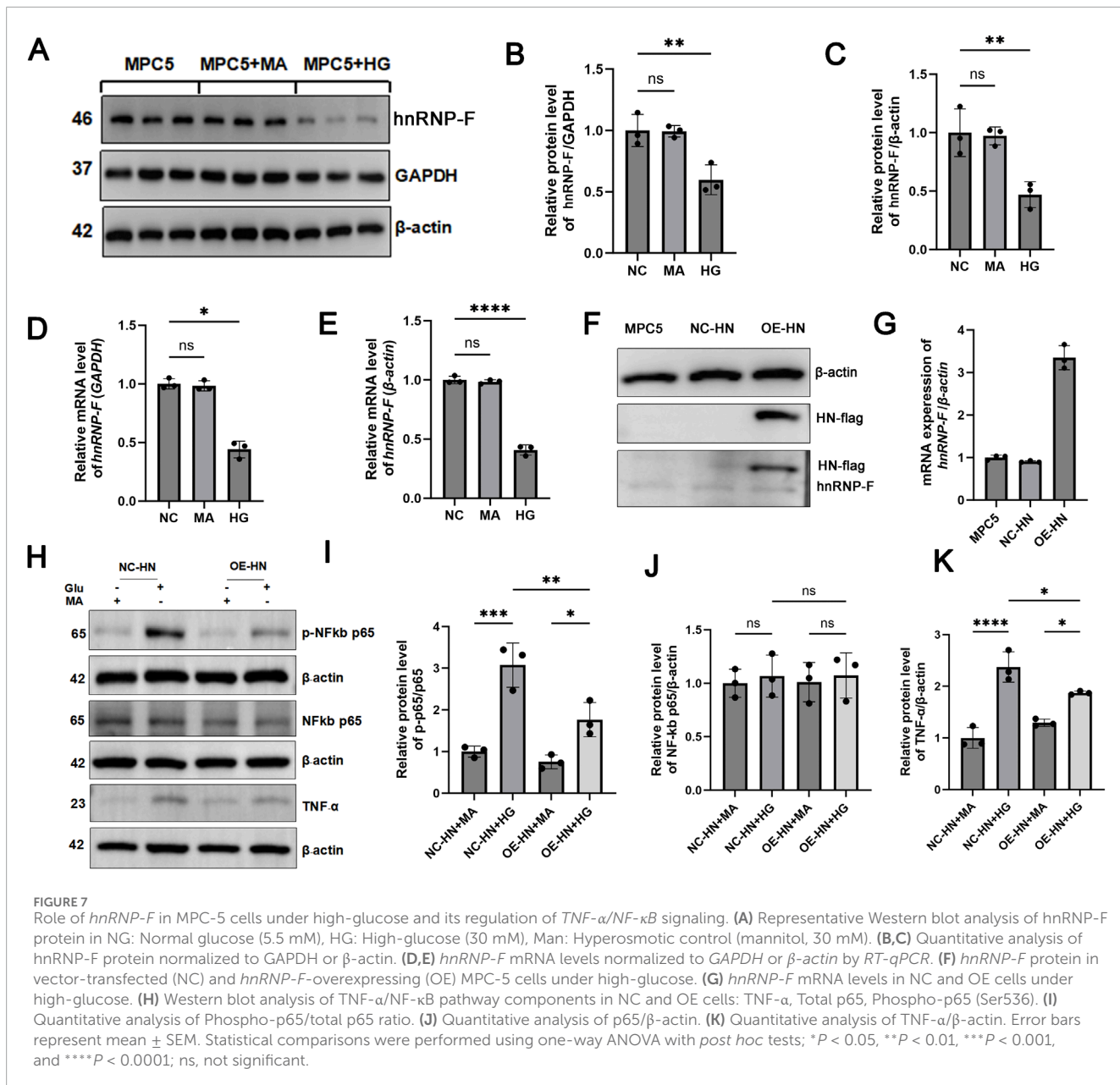
may have facilitated the upregulation of these genes in the *db/db* mouse model.

3.7 *hnRNP-F* overexpression exerts anti-inflammatory effects in MPC5 cells under HG conditions

Under HG conditions, MPC-5 cells demonstrated a significant reduction in *hnRNP-F* protein levels ($^{**}P < 0.01$), with minimal correlation to hyperosmolarity induced by mannitol (Figures 7A–E). In cells stably transfected to overexpress *hnRNP-F* (validated by immunoblotting) (Figures 7F,G), $\text{TNF-}\alpha$ expression was significantly attenuated in HG conditions ($^{*}P < 0.05$) (Figures 7H,K), and $\text{NF-}\kappa\text{B}$ p-p65 phosphorylation was notably suppressed ($^{**}P < 0.01$) (Figures 7H–J).

3.8 Effect of LPS on *hnRNP-F* expression and anti-inflammatory effects of *hnRNP-F* overexpression in LPS-treated MPC5 cells

Under LPS-induced inflammatory conditions, *hnRNP-F* protein levels were significantly decreased in both HK-2 cells and MPC-5 podocytes ($^{*}P < 0.001$; $P < 0.01$; Figures 8A–F). In MPC-5 cells stably transfected to overexpress *hnRNP-F*, $\text{TNF-}\alpha$ expression was markedly attenuated ($^{*}P < 0.05$) (Figure 8I), and $\text{NF-}\kappa\text{B}$ p-p65/p65 was significantly suppressed ($^{**}P < 0.01$) (Figures 8G,H) under LPS exposure.



3.9 *hnRNP-F* is physically associated with *ZFP36* to form a complex that regulates gene expression and alternative splicing

To elucidate the mechanistic role of *hnRNP-F* in transcriptional repression, we conducted Co-IP experiments to examine the *hnRNP-F* interactome *in vivo*. In these experiments, HK-2 cells were engineered to stably overexpress *hnRNP-F*. Total protein lysates were subjected to immunoprecipitation using antibodies specific to *hnRNP-F*, followed by WB with antibodies targeting *ZFP36*, *HNRNPH*, and *FOXP3* (Figure 9). The Co-IP analysis using *hnRNP-F* antibodies, followed by WB with *ZFP36* antibodies, demonstrated a physical association between *hnRNP-F* and *ZFP36*. The *ZFP36* gene, also known as tristetraprolin (TTP), is a crucial RNA-binding

protein that plays a vital role in various biological processes. *ZFP36* modulates mRNA stability through its interaction with AU-rich elements (AREs) within mRNA, consequently affecting gene expression and cellular function (Makita et al., 2021). Furthermore, empirical evidence suggests that *ZFP36* plays a substantial role in the regulation of alternative splicing (Tu et al., 2019; Chan et al., 2025). We speculate that *hnRNP-F* and *ZFP36* form a complex that regulates gene expression and alternative splicing.

4 Discussion

The pathophysiology of DKD involves multiple pathways, such as hemodynamic, metabolic, and inflammatory pathways. Targeting inflammatory and fibrotic pathways may have important therapeutic

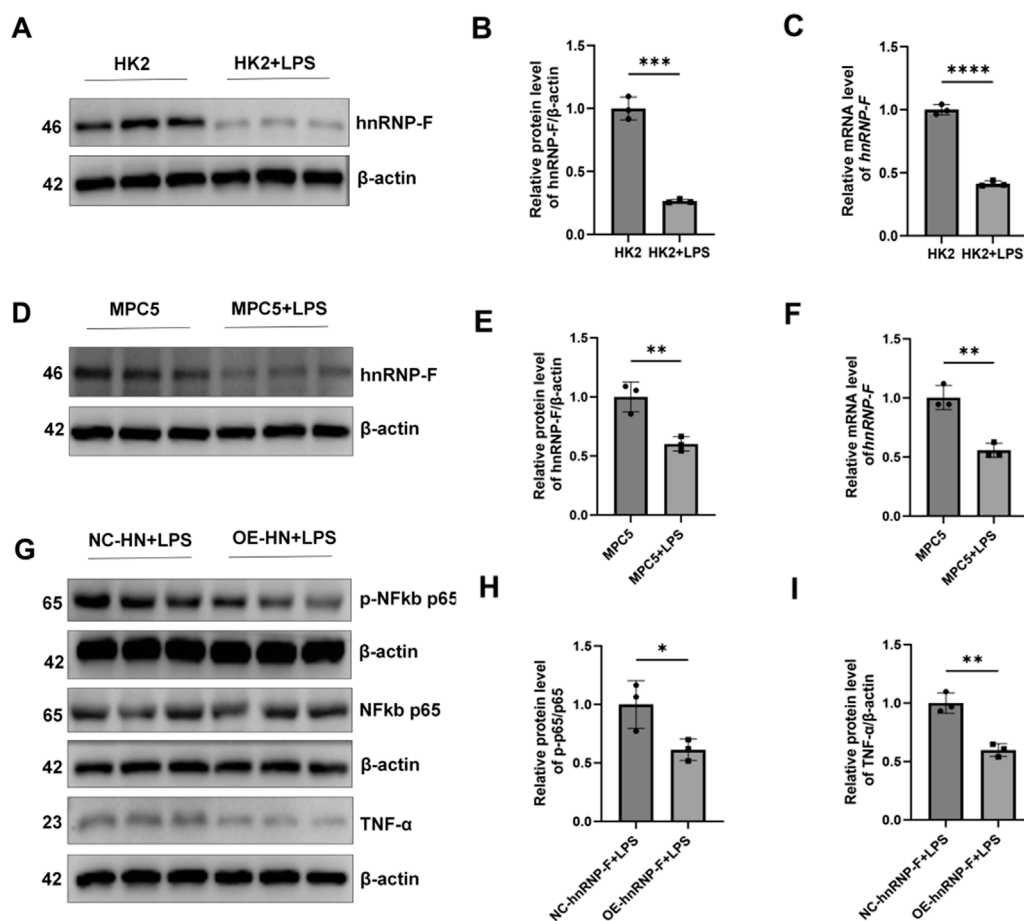


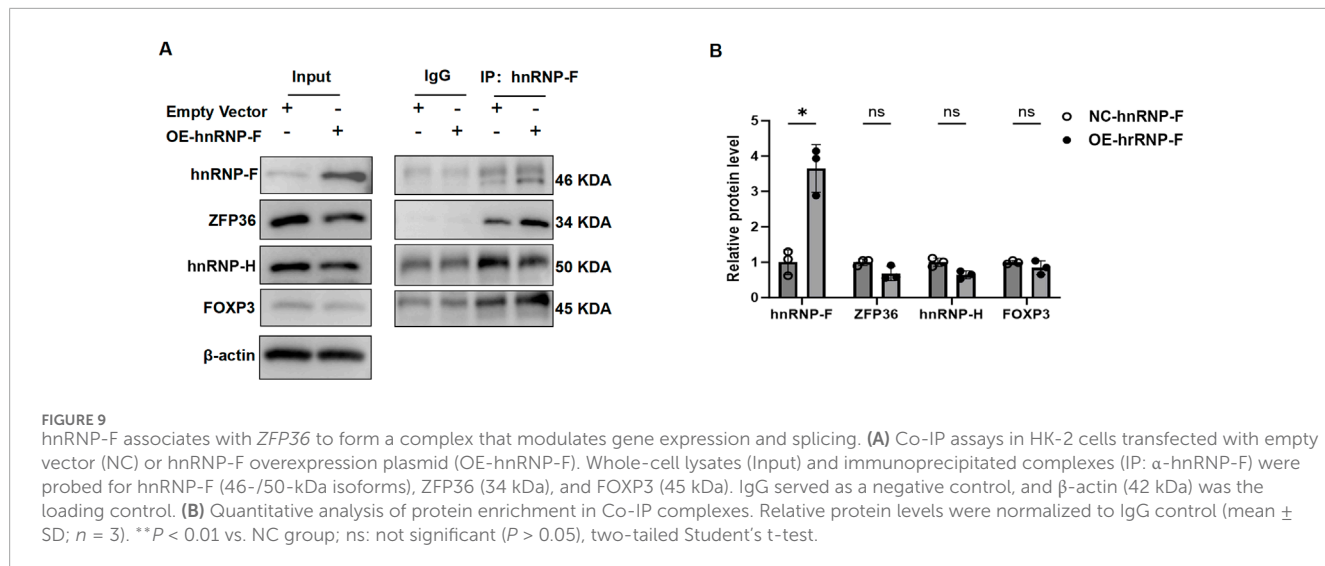
FIGURE 8

Expression of *hnRNP-F* in HK2 cells and MPC-5 cells under LPS conditions and its regulation of the TNF- α /NF- κ B signaling pathway in MPC-5 cells. (A) Representative immunoblot images of *hnRNP-F* protein expression in HK-2 cells under LPS conditions (10 μ g/mL) and normal conditions. (B) *hnRNP-F* mRNA levels in HK-2 cells under normal and LPS conditions were quantified by RT-qPCR and normalized to β -actin. (C) Quantitative analysis of *hnRNP-F* protein normalized to β -actin in MPC5 cells under LPS conditions (45 μ g/mL) and normal conditions. (D) Quantitative analysis of *hnRNP-F* protein normalized to β -actin in MPC5 cells under normal and LPS conditions. (E) Quantitative analysis of *hnRNP-F* mRNA levels in MPC5 cells under normal and LPS conditions were quantified by RT-qPCR and normalized to β -actin. (F) Western blot of TNF- α /NF- κ B pathway components in NC-*hnRNP-F* and OE-*hnRNP-F* MPC5 cells: TNF- α , total p65, phosphorylated p65 (Ser536). (G) Quantitative analysis of the phosphorylated p65/total p65 ratio in MPC5 cells under basal and LPS conditions. (H) Quantitative analysis of TNF- α /β-actin in MPC5 cells under basal and LPS conditions. Error bars represent mean \pm SEM. Statistical comparisons were performed using one-way ANOVA with post hoc tests; * P < 0.05, ** P < 0.01, *** P < 0.001, **** P < 0.0001; ns, not significant.

implications in DKD research (Matoba et al., 2019). Therefore, it is necessary to further investigate its molecular regulatory mechanism in cells associated with DKD to provide new ideas for finding new therapeutic targets for DKD.

As an RNA-binding protein, *hnRNP-F* is capable of binding to mRNA and participating in the post-transcriptional regulation of target genes, and it is known to modulate the expression of target genes. Abnormal expression of *hnRNP-F* has been reported to have a significant effect on the progression of diabetic nephropathy, and high expression of *hnRNP-F* may have a better protective effect. In patients with type 2 diabetes, the protein levels of *hnRNP-F* have significantly decreased in renal cortex tissues, but the role of *hnRNP-F* in renal tubular epithelial cell mechanisms remains unclear (Liao et al., 2024). RNA-seq analysis in this study demonstrated that *hnRNP-F* broadly modulates high-glucose-induced differential gene expression and alternative splicing in

HK-2 cells. Downregulation of *hnRNP-F* expression under HG conditions or in DKD was subsequently confirmed across HK-2 cells, MPC5 cells, and *db/db* mouse models. Furthermore, lentivirus-mediated *hnRNP-F* overexpression in MPC5 cells significantly suppressed the TNF- α /NF- κ B signaling pathway. The expression and synthesis of TNF- α , a potent inflammatory factor, are not only limited to hematopoietic cells, but also can be produced by renal intrinsic cells, such as mesangial cells, endothelial cells, tubular epithelial cells, etc. (Jevnikar et al., 1991; Sugimoto et al., 1999). TNF- α plays an activating role in renal intrinsic cells, including a second messenger system, transcription factors, and cytokines, and participates in the synthesis of inflammatory mediators and tissue-compatible complexes (Vielhauer et al., 2005). It has been demonstrated that insulin-resistant diabetic patients have increased serum levels of TNF- α (Iwata et al., 2001), and the levels of TNF- α in the blood or glomerular cells are considered to correlate with



the damage to the tethered cells in patients with DKD. Being a pleiotropic transcription factor, *NF- κ B* is a regulatory hub for thylakoid cells to express a variety of immune-inflammation-related genes, and is intimately implicated in thylakoid cell proliferation and secretion of inflammatory factors (Evans et al., 2002). Numerous studies have shown that *NF- κ B* may accelerate the progression of DKD by regulating inflammation; for example, it has been shown that *NF- κ B* mediates high-glucose-induced inflammatory response and ECM accumulation in glomerular mesangial cells (Chen et al., 2016; Liu et al., 2019).

We considered that the significant downregulation of *CXCL8*, *IL6*, *GDF15*, *PTX3*, and *TFPI2* warranted additional focus. Existing studies have reported that inhibition of *CXCL8* attenuates high-glucose-induced renal tubular cell-mediated inflammation and apoptosis in diabetic kidney disease (Bai et al., 2022). Significantly, activation of *CXCL8* has been demonstrated to heighten *TNF- α* -induced inflammatory responses (Huang et al., 2018). *IL-6* signaling is known to be involved in the core inflammatory response in the progression of DKD (Feigerlová and Battaglia-Hsu, 2017). As is known, *TNF- α* inhibits the transcription factors resulting in the production of *IL-6* (Tanaka et al., 2014). Growth differentiation factor-15 (*GDF-15*) increases the likelihood of DKD by affecting reno-protective factors with anti-inflammatory activity (Delrue et al., 2023). *GDF-15* inhibits inflammation by reducing the infiltration of inflammatory cells, diminishing the secretion of cytokines and chemokines, and attenuating macrophage and T cell activity to suppress the release of *TNF- α* , *IL-6*, and *IL-1 β* (Tang et al., 2024). In addition, it has been shown that *TNF- α* could increase the transcriptional activity of *GDF-15* by potentiating multiple signal transduction pathways, especially the classical *NF- κ B* and *MAPK* pathways (Adela et al., 2015).

Two other genes, *PTX3* and *TFPI2*, were also involved in the DKD pathological process. *PTX3* induces mitochondrial dysfunction and renal tubular cell senescence via β -linker activation, leading to renal fibrosis (Luo et al., 2023). It was reported that *TFPI2* can regulate the endothelial–mesenchymal transition and the *TGF- β 2* signaling pathway and is a potential promoter of DKD pathogenesis (Guan et al., 2022). We also downloaded the CLIP-seq data of *hnRNP-F* and found that *hnRNP-F* and lncRNA *SNHG1*

had the potential to combine. Meanwhile, the expression of lncRNA *SNHG1* was downregulated after *hnRNP-F* overexpression. *SNHG1* is an annotated lncRNA, which is mainly localized in the nucleus. It is well established that *SNHG1* interacts with the promoter regions of its downstream genes to enhance their expression (Li et al., 2020; Sun et al., 2017). The present study demonstrates that overexpression of *hnRNP-F* results in decreased levels of *SNHG1* expression. Additionally, the expression of certain *TNF α* -related genes is suppressed following *hnRNP-F* overexpression. These findings suggest a potential interaction between *hnRNP-F* and *SNHG1* in regulating the transcription of these target genes.

Our present experiments revealed that *hnRNP-F* combined with lncRNA *SNHG1* in high-glucose-induced renal tubular epithelial cells significantly reduced the expression of genes associated with the *TNF α /NF κ B* signaling pathway or with DKD pathogenesis (Figure 3). The mechanism of this transcriptional repression requires further investigation. Undoubtedly, previous studies indicate that *hnRNP-F* interacts with multiple proteins, including *hnRNP-H*, *FOXP3*, and tristetraprolin (*TTP*, also known as *ZFP36*) (Reznik et al., 2014). Co-IP assays performed in HK2 cells confirmed a physical interaction between *hnRNP-F* and *ZFP36* (* $P < 0.05$ vs. IgG control). However, no interaction was detected between *hnRNP-F* and *FOXP3*. While *hnRNP-H* co-precipitated with *hnRNP-F*, its comigration with the antibody heavy chain (~50 kDa) precluded definitive assessment of this interaction. Notably, overexpression of *hnRNP-F* did not significantly alter the protein levels of *ZFP36*, *FOXP3*, or *hnRNP-H*, as determined by densitometric analysis (Figure 10). A prior study suggested that *hnRNP-F* acts as a co-factor with *TTP* to increase ARE-mRNA decay. The current study hypothesizes that *hnRNP-F* and *TTP* form a complex mediated by *SNHG1* to regulate gene expression. Nevertheless, further experimental evidence is necessary to substantiate this conclusion.

hnRNP-F, as a coregulator of alternative splicing, always interacts with other RNA-binding proteins, including *RBM41*. We found that *hnRNP-F* overexpression notably promotes several alternative RNA-binding protein splicings. We observed that *hnRNP-F*-dependent alternative splicing of *RBM41* generates a short isoform in *hnRNP-F* overexpression cells. *RBM41* is the paralog

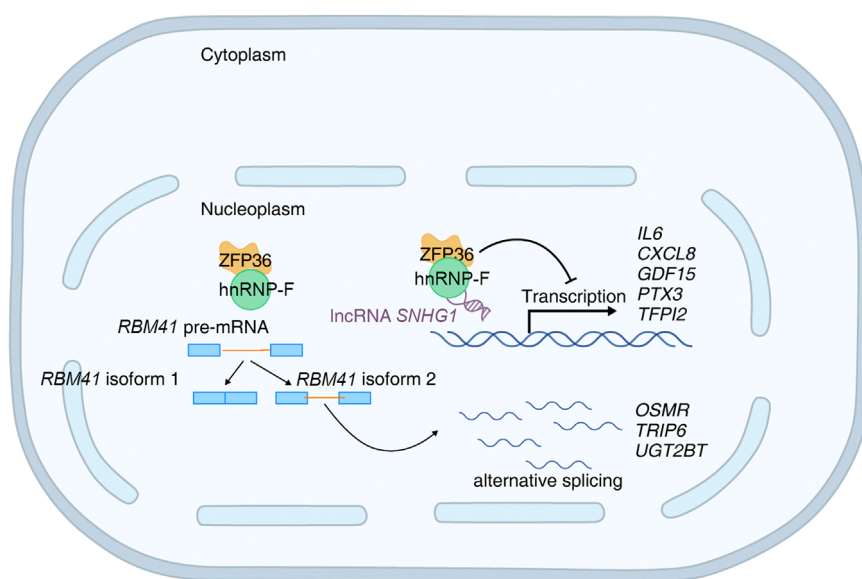


FIGURE 10
Schematic diagram of hnRNP-F-mediated regulation of gene expression and alternative splicing in high-glucose.

of U11/U12-65K, a known unique component of the U11/U12 di-snRNP. Both proteins utilize their highly similar C-terminal RRM domains to bind the 3'-terminal stem-loops in U12 and U6atac snRNAs with comparable affinity. Recent studies identify RBM41 as a novel, unique protein component of the minor spliceosome, functioning in post-splicing steps and the disassembly process of the minor spliceosome (Norppa et al., 2024; Taira et al., 2025). It is speculated that *hnRNP-F* may affect the alternative splicing of RBM41, thereby influencing the overall post-transcriptional regulatory pattern within the cell.

We also found that *hnRNP-F* overexpression significantly alters variable exons of *OSMR* and *UGT2B7*. *OSMR* is a receptor for *OSM*, and *OSM* signaling plays a role in fibrosis, including inflammation, vascular dysfunction, and fibroblast activation (Stawski and Trojanowska, 2019). Miroslav Dostalek et al. discovered that diabetes reduces *UGT2B7* enzymatic activity in the kidney (Dostalek et al., 2011).

hnRNP-F also affects the inclusion or deletion of exons in some genes, resulting in transcripts of different lengths, like gene *TRIP6* and *IRF3*. *TRIP6* mediates inflammatory response and fibrosis in diabetic nephropathy (Lin et al., 2021). As a key molecule in the interferon gene/interferon regulatory factor 3 (STING/IRF3) signaling pathway, *IRF3* is involved in mediating the inflammatory response at different stages of DKD progression (El-Deeb et al., 2023). Analysis of CLIP-seq data from *hnRNP-F* showed that *hnRNP-F* specifically binds to some *hnRNP* family proteins and splicing factors. Based on the above results, we speculated that *hnRNP-F* may mediate variable splicing in high-glucose-induced HK2 cells through interaction with *hnRNP* family proteins (Figure 5).

In summary, *hnRNP-F* could have dual functions in mRNA transcriptional and post-transcriptional levels. We find that *hnRNP-F* may bind with IncRNA *SNHG1* to negatively regulate the transcription of genes involved in the *TNF α /NF κ B* signaling

pathway. Interestingly, *hnRNP-F* also regulates the alternative splicing of *hnRNP* proteins and splicing factors. This finding suggests that *hnRNP-F* may play a role in DKD by regulating the differential expression and variable splicing of genes associated with diabetic nephropathy, especially genes associated with inflammatory response; however, its exact mechanism requires further experimental verification.

Data availability statement

The data presented in the study are deposited in the GEO repository, accession numbers GSE273001 and GSE299230.

Ethics statement

Ethical approval was not required for the studies on humans in accordance with the local legislation and institutional requirements because only commercially available established cell lines were used. The animal study was approved by the Animal Ethics Committee of Hubei University of Chinese Medicine (Approval No. HUCMS00303837). The study was conducted in accordance with the local legislation and institutional requirements.

Author contributions

LW: Formal analysis, Funding acquisition, Project administration, Supervision, Writing – original draft, and Writing – review and editing. HL: Data curation, Formal analysis, Methodology, Software, Validation, Visualization, Writing – original draft. XG: Data curation, Software, Visualization, Investigation, Writing – original draft. XW: Conceptualization, Funding

acquisition, Project administration, Resources, Supervision, Writing – review and editing.

Funding

The author(s) declare that financial support was received for the research and/or publication of this article. This study was supported by the Joint Fund Project of Hubei Provincial Natural Science Foundation (2022CFD021), the Research Project of Hubei Provincial Administration of Traditional Chinese Medicine (ZY2023F003), and the National Natural Science Foundation of China (82374384).

Conflict of interest

The authors declare that the research was conducted in the absence of any commercial or financial relationships that could be construed as a potential conflict of interest.

References

Adela, R., and Banerjee, S. K. (2015). GDF-15 as a target and biomarker for diabetes and cardiovascular diseases: a translational prospective. *J. Diabetes Res.* 2015, 490842. doi:10.1155/2015/490842

Bai, Y., Li, H., and Dong, J. (2022). Up-regulation of miR-20a weakens inflammation and apoptosis in high-glucose-induced renal tubular cell mediating diabetic kidney disease by repressing CXCL8 expression. *Arch. Physiol. Biochem.* 128 (6), 1603–1610. doi:10.1080/13813455.2020.1785506

Barrera-Chimal, J., and Jaisser, F. (2020). Pathophysiologic mechanisms in diabetic kidney disease: a focus on current and future therapeutic targets. *Diabetes Obes. Metab.* 22 (Suppl. 1), 16–31. doi:10.1111/dom.13969

Chan, T. S., Lee, K. L., Hung, C. S., Chiang, H. P., Chung, C. C., and Liang, Y. C. (2025). ZFP36L1 and ZFP36L2 reduce cyclin D1 expression by decreasing expression of E2F1 and long 3'UTR isoform of CCND1 transcripts. *Mol. Cell Biochem.* 480 (3), 1685–1699. doi:10.1007/s11010-024-05087-w

Chen, J., Hou, X. F., Wang, G., Zhong, Q. X., Liu, Y., Qiu, H. H., et al. (2016). Terpene glycoside component from Moutan Cortex ameliorates diabetic nephropathy by regulating endoplasmic reticulum stress-related inflammatory responses. *J. Ethnopharmacol.* 193, 433–444. doi:10.1016/j.jep.2016.09.043

Chen, Y., Lee, K., Ni, Z., and He, J. C. (2020). Diabetic kidney disease: challenges, advances, and opportunities. *Kidney Dis. (Basel)* 6 (4), 215–225. doi:10.1159/000506634

Cheng, C., Liu, L., Bao, Y., Yi, J., Quan, W., Xue, Y., et al. (2021). SUVA: splicing site usage variation analysis from RNA-seq data reveals highly conserved complex splicing biomarkers in liver cancer. *RNA Biol.* 18 (Suppl. 1), 157–171. doi:10.1080/15476286.2021.1940037

Darshi, M., Kugathasan, L., Maity, S., Sridhar, V. S., Fernandez, R., Limonte, C. P., et al. (2024). Glycolytic lactate in diabetic kidney disease. *JCI Insight* 9 (11), e168825. doi:10.1172/jci.insight.168825

Delrue, C., Speeckaert, R., Delanghe, J. R., and Speeckaert, M. M. (2023). Growth differentiation factor 15 (GDF-15) in kidney diseases. *Adv. Clin. Chem.* 114, 1–46. doi:10.1016/bs.acc.2023.02.003

Dostalek, M., Court, M. H., Hazarika, S., and Akhlaghi, F. (2011). Diabetes mellitus reduces activity of human UDP-glucuronosyltransferase 2B7 in liver and kidney leading to decreased formation of mycophenolic acid acyl-glucuronide metabolite. *Drug Metab. Dispos.* 39 (3), 448–455. doi:10.1124/dmd.110.036608

El-Deeb, O. S., Hafez, Y. M., Eltokhy, A. K., Awad, M. M., El-Shaer, R. A. A., Abdel Ghafar, M. T., et al. (2023). Stimulator of interferon genes/interferon regulatory factor 3 (STING-IRF3) and inflammasome-activation mediated pyroptosis biomarkers: a network of integrated pathways in diabetic nephropathy. *J. Diabetes Metab. Disord.* 22 (2), 1471–1480. doi:10.1007/s40200-023-01270-w

Evans, J. L., Goldfine, I. D., Maddux, B. A., and Grodsky, G. M. (2002). Oxidative stress and stress-activated signaling pathways: a unifying hypothesis of type 2 diabetes. *Endocr. Rev.* 23 (5), 599–622. doi:10.1210/er.2001-0039

Feigerlová, E., and Battaglia-Hsu, S. F. (2017). IL-6 signaling in diabetic nephropathy: from pathophysiology to therapeutic perspectives. *Cytokine Growth Factor Rev.* 37, 57–65. doi:10.1016/j.cytogfr.2017.03.003

Ghosh, A., Zhao, S., Lo, C. S., Maachi, H., Chenier, I., Lateef, M. A., et al. (2019). Heterogeneous nuclear ribonucleoprotein F mediates insulin inhibition of Bcl2-Modifying factor expression and tubulopathy in diabetic kidney. *Sci. Rep.* 9 (1), 6687. doi:10.1038/s41598-019-43218-2

Guan, G., Xie, J., Dai, Y., and Han, H. (2022). TFP12 suppresses the interaction of TGF- β 2 pathway regulators to promote endothelial-mesenchymal transition in diabetic nephropathy. *J. Biol. Chem.* 298 (3), 101725. doi:10.1016/j.jbc.2022.101725

Heinz, S., Benner, C., Spann, N., Bertolino, E., Lin, Y. C., Laslo, P., et al. (2010). Simple combinations of lineage-determining transcription factors prime cis-regulatory elements required for macrophage and B cell identities. *Mol. Cell* 38 (4), 576–589. doi:10.1016/j.molcel.2010.05.004

Huang, H., Zhang, J., Harvey, S. E., Hu, X., and Cheng, C. (2017). RNA G-quadruplex secondary structure promotes alternative splicing via the RNA-binding protein hnRNPf. *Genes Dev.* 31 (22), 2296–2309. doi:10.1101/gad.305862.117

Huang, Z., Du, G., Huang, X., Han, L., Han, X., Xu, B., et al. (2018). The enhancer RNA lnc-SLC4A1-1 epigenetically regulates unexplained recurrent pregnancy loss (URPL) by activating CXCL8 and NF- κ B pathway. *EBioMedicine* 38, 162–170. doi:10.1016/j.ebiom.2018.11.015

Iwata, M., Haruta, T., Usui, I., Takata, Y., Takano, A., Uno, T., et al. (2001). Pioglitazone ameliorates tumor necrosis factor-alpha-induced insulin resistance by a mechanism independent of adipogenic activity of peroxisome proliferator-activated receptor-gamma. *Diabetes* 50 (5), 1083–1092. doi:10.2337/diabetes.50.5.1083

Jevnikar, A. M., Brennan, D. C., Singer, G. G., Heng, J. E., Maslinski, W., Wuthrich, R. P., et al. (1991). Stimulated kidney tubular epithelial cells express membrane associated and secreted TNF alpha. *Kidney Int.* 40 (2), 203–211. doi:10.1038/ki.1991.201

Kim, D., Langmead, B., and Salzberg, S. L. (2015). HISAT: a fast spliced aligner with low memory requirements. *Nat. methods* 12 (4), 357–360. doi:10.1038/nmeth.3317

Ladd, A. N. (2016). New insights into the role of RNA-Binding proteins in the regulation of heart development. *Int. Rev. Cell Mol. Biol.* 324, 125–185. doi:10.1016/bs.ircmb.2015.12.009

Li, B., Li, A., You, Z., Xu, J., and Zhu, S. (2020). Epigenetic silencing of CDKN1A and CDKN2B by SNHG1 promotes the cell cycle, migration and epithelial-mesenchymal transition progression of hepatocellular carcinoma. *Cell Death Dis.* 11 (10), 823. doi:10.1038/s41419-020-03031-6

Liao, M. C., Lo, C. S., Pang, Y. C., Yang, W. X., Su, K., Zhao, X. P., et al. (2024). Heterogeneous nuclear ribonucleoprotein F deficiency in mouse podocyte promotes podocytopathy mediated by methyltransferase-like 14 nuclear translocation resulting in Sirtuin 1 gene inhibition. *Transl. Res.* 267, 1–9. doi:10.1016/j.trsl.2024.01.002

Generative AI statement

The author(s) declare that no Generative AI was used in the creation of this manuscript.

Publisher's note

All claims expressed in this article are solely those of the authors and do not necessarily represent those of their affiliated organizations, or those of the publisher, the editors and the reviewers. Any product that may be evaluated in this article, or claim that may be made by its manufacturer, is not guaranteed or endorsed by the publisher.

Supplementary material

The Supplementary Material for this article can be found online at: <https://www.frontiersin.org/articles/10.3389/fphys.2025.1475441/full#supplementary-material>

Lin, Y. C., Chang, Y. H., Yang, S. Y., Wu, K. D., and Chu, T. S. (2018). Update of pathophysiology and management of diabetic kidney disease. *J. Formos. Med. Assoc.* 117 (8), 662–675. doi:10.1016/j.jfma.2018.02.007

Lin, Y., Shao, Z., Zhao, M., Li, J., and Xu, X. (2021). PTPN14 deficiency alleviates podocyte injury through suppressing inflammation and fibrosis by targeting TRIP6 in diabetic nephropathy. *Biochem. Biophys. Res. Commun.* 550, 62–69. doi:10.1016/j.bbrc.2020.12.030

Liu, Z., Han, Y., Zhao, F., Zhao, Z., Tian, J., and Jia, K. (2019). Nobiletin suppresses high-glucose-induced inflammation and ECM accumulation in human mesangial cells through STAT3/NF- κ B pathway. *J. Cell Biochem.* 120 (3), 3467–3473. doi:10.1002/jcb.27621

Lo, C. S., Shi, Y., Chang, S. Y., Abdo, S., Chenier, I., Filep, J. G., et al. (2015). Overexpression of heterogeneous nuclear ribonucleoprotein F stimulates renal Ace-2 gene expression and prevents TGF- β 1-induced kidney injury in a mouse model of diabetes. *Diabetologia* 58 (10), 2443–2454. doi:10.1007/s00125-015-3700-y

Love, M. I., Huber, W., and Anders, S. (2014). Moderated estimation of fold change and dispersion for RNA-seq data with DESeq2. *Genome Biol.* 15 (12), 550–21. doi:10.1186/s13059-014-0550-8

Luo, P., Zhang, H., Liang, Y., Li, X., Wen, Z., Xia, C., et al. (2023). Pentraxin 3 plays a key role in tubular cell senescence and renal fibrosis through inducing β -catenin signaling. *Biochim. Biophys. Acta Mol. Basis Dis.* 1869 (7), 166807. doi:10.1016/j.bbadic.2023.166807

Lytvyn, Y., Bjornstad, P., van Raalte, D. H., Heerspink, H. L., and Cherney, D. Z. I. (2020). The new biology of diabetic kidney disease—mechanisms and therapeutic implications. *Endocr. Rev.* 41 (2), 202–231. doi:10.1210/endrev/bnz010

Makita, S., Takatori, H., and Nakajima, H. (2021). Post-transcriptional regulation of immune responses and inflammatory diseases by RNA-binding ZFP36 family proteins. *Front. Immunol.* 12, 711633. doi:10.3389/fimmu.2021.711633

Matoba, K., Takeda, Y., Nagai, Y., Kawanami, D., Utsunomiya, K., and Nishimura, R. (2019). Unraveling the role of inflammation in the pathogenesis of diabetic kidney disease. *Int. J. Mol. Sci.* 20 (14), 3393. doi:10.3390/ijms20143393

Norppa, A. J., Chowdhury, I., van Rooijen, L. E., Ravantti, J. J., Snel, B., Varjosalo, M., et al. (2024). Distinct functions for the paralogous RBM41 and U11/U12-65K proteins in the minor spliceosome. *Nucleic Acids Res.* 52 (7), 4037–4052. doi:10.1093/nar/gkae070

Reznik, B., Clement, S. L., and Lykke-Andersen, J. (2014). hnRNP F complexes with tristetraprolin and stimulates ARE-mRNA decay. *PLoS One* 9 (6), e100992. doi:10.1371/journal.pone.0100992

Smith, J. M., Sandow, J. J., and Webb, A. I. (2021). The search for RNA-binding proteins: a technical and interdisciplinary challenge. *Biochem. Soc. Trans.* 49 (1), 393–403. doi:10.1042/BST20200688

Stawski, L., and Trojanowska, M. (2019). Oncostatin M and its role in fibrosis. *Connect. Tissue Res.* 60 (1), 40–49. doi:10.1080/03008207.2018.1500558

Sugimoto, H., Shikata, K., Wada, J., Horiuchi, S., and Makino, H. (1999). Advanced glycation end products-cytokine-nitric oxide sequence pathway in the development of diabetic nephropathy: aminoguanidine ameliorates the overexpression of tumour necrosis factor-alpha and inducible nitric oxide synthase in diabetic rat glomeruli. *Diabetologia* 42 (7), 878–886. doi:10.1007/s001250051241

Sun, Y., Wei, G., Luo, H., Wu, W., Skogerbo, G., Luo, J., et al. (2017). The long noncoding RNA SNHG1 promotes tumor growth through regulating transcription of both local and distal genes. *Oncogene* 36 (49), 6774–6783. doi:10.1038/onc.2017.286

Taira, Y., Zhu, L., and Fukunaga, R. (2025). RNA-binding protein Miso/CG44249 is crucial for minor splicing during oogenesis in *Drosophila*. *RNA* 31 (6), 822–835. doi:10.1261/rna.080311.124

Tanaka, T., Narasaki, M., and Kishimoto, T. (2014). IL-6 in inflammation, immunity, and disease. *Cold Spring Harb. Perspect. Biol.* 6 (10), a016295. doi:10.1101/cshperspect.a016295

Tang, Y., Liu, T., Sun, S., Peng, Y., Huang, X., Wang, S., et al. (2024). Role and mechanism of growth differentiation factor 15 in chronic kidney disease. *J. Inflamm. Res.* 17, 2861–2871. doi:10.2147/JIR.S451398

Trapnell, C., Williams, B. A., Pertea, G., Mortazavi, A., Kwan, G., Van Baren, M. J., et al. (2010). Transcript assembly and quantification by RNA-Seq reveals unannotated transcripts and isoform switching during cell differentiation. *Nat. Biotechnol.* 28 (5), 511–515. doi:10.1038/nbt.1621

Tu, Y., Wu, X., Yu, F., Dang, J., Wang, J., Wei, Y., et al. (2019). Tristetraprolin specifically regulates the expression and alternative splicing of immune response genes in HeLa cells. *BMC Immunol.* 20 (1), 13. doi:10.1186/s12865-019-0292-1

Tuttle, K. R., Agarwal, R., Alpers, C. E., Bakris, G. L., Brosius, F. C., Kolkhof, P., et al. (2022). Molecular mechanisms and therapeutic targets for diabetic kidney disease. *Kidney Int.* 102 (2), 248–260. doi:10.1016/j.kint.2022.05.012

Vielhauer, V., Stavrakis, G., and Mayadas, T. N. (2005). Renal cell-expressed TNF receptor 2, not receptor 1, is essential for the development of glomerulonephritis. *J. Clin. Invest.* 115 (5), 1199–1209. doi:10.1172/JCI23348

Wang, L., Zhu, G., and Wang, X. (2021). Renal protective effects of Shenyuan Granules on db/db diabetic nephropathy mice based on TGF- β 1/Egr1 signaling pathway regulated by Klotho. *China J. Tradit. Chin. Med. Pharm.* 36 (08), 5033–5036.

Wu, B., Su, S., Patil, D. P., Liu, H., Gan, J., Jaffrey, S. R., et al. (2018). Molecular basis for the specific and multivariant recognitions of RNA substrates by human hnRNP A2/B1. *Nat. Commun.* 9 (1), 420. doi:10.1038/s41467-017-02770-z

Xia, H., Chen, D., Wu, Q., Wu, G., Zhou, Y., Zhang, Y., et al. (2017). CELF1 preferentially binds to exon-intron boundary and regulates alternative splicing in HeLa cells. *Biochim. Biophys. Acta Gene Regul. Mech.* 1860 (9), 911–921. doi:10.1016/j.bbagr.2017.07.004

Xie, C., Mao, X., Huang, J., Ding, Y., Wu, J., Dong, S., et al. (2011). KOBAS 2.0: a web server for annotation and identification of enriched pathways and diseases. *Nucleic acids Res.* 39 (Suppl. 1_2), W316–W322. doi:10.1093/nar/gkr483

Zhou, A. X., Jeansson, M., He, L., Wigge, L., Tonelius, P., Tati, R., et al. (2024). Renal endothelial single-cell transcriptomics reveals spatiotemporal regulation and divergent roles of differential gene transcription and alternative splicing in Murine Diabetic Nephropathy. *Int. J. Mol. Sci.* 25 (8), 4320. doi:10.3390/ijms25084320